Applied Nanoscience (2023) 13:5865–5875
https://doi.org/10.1007/s13204-023-02812-7

ORIGINAL ARTICLE

Green chemistry approach for silver nanoparticles synthesis from *Halimeda macroloba* and their potential medical and environmental applications

G. Lavanya[1] · K. Anandaraj[1] · M. Gopu[2] · K. Selvam[2] · T. Selvankumar[2] · M. Govarthanan[3,4] · P. Kumar[5]

Received: 8 November 2022 / Accepted: 27 February 2023 / Published online: 12 April 2023

Abstract

This study aims to synthesize silver nanoparticles (AgNPs) using *Halimeda macroloba* extract and assess their anticancer and photocatalytic properties. Ultraviolet–visible spectrophotometry (UV–visible), Fourier transform infrared (FT-IR) spectroscopy, Transmission electron microscope (TEM), scanning electron microscope-energy-dispersive spectroscopy (SEM–EDX), X-ray photoelectron spectroscopy (XPS), and particle-size distribution (PSD) were used to characterize the synthesized AgNPs. The green-synthesized AgNPs to be spherical in shape with a size of about 50–100 nm. The half-maximal inhibitory concentration (IC_{50}) for AgNPs was determined to be 89.5 g/mL against the human hepatoma cell line (Huh-7). Fluorescent microscopy was used to evaluate the morphological alterations of Huh-7 cells stained with acridine orange/ethidium bromide (AO/EtBr), 2′-7′dichlorofluorescin diacetate (DCFH-DA), and rhodamine 123. Meanwhile, AgNPs exhibited 91.35% photocatalytic activity against methylene blue (MB) after 100 min of exposure to sunlight. Therefore, AgNPs have a strong potential for usage in anticancer activities and photocatalytic organic pollutant destruction.

Keywords Green seaweeds · *Halimeda macroloba* · Silver nanoparticles · Anticancer activity · Photocatalytic activity

Introduction

In decades past, nanotechnology was indeed a notable branch of contemporary research dealing with the manipulation, synthesis, and design of particles with 1–100 nm dimensions. Nanoparticles (NPs) are characterized by their small size and increased surface area, and they are utilized in numerous industries, including cosmetics, food industries, environmental bioremediation, optics, electrical, textile, catalysts, light emitters, photocatalytic, biosensors, energy research, drug delivery, and biological sciences (Ashraf et al. 2019; Behzad et al. 2021; Paiva-Santos et al. 2021; Sana et al. 2021; Wang et al. 2021; de Jesus et al. 2021; Seitkalieva et al. 2021; Dawood et al. 2022; Hojjati-Najafabadi et al. 2022). The various types of noble metal nanoparticles, including copper, zinc, titanium, magnesium, nickel, iron, silver, and gold. Among them, silver NPs are widely used in the sectors of cosmetics, nanomedicine, photocatalytic, food processing, biomedical imaging, antibacterial activities, and more due to their unusual stability, conductivity, and targeted medication delivery (Aravinthan et al. 2015; Chinnappan et al. 2018; Balakrishnan et al. 2020; Gopu et al.

✉ K. Anandaraj
kanandaraj2010@gmail.com

✉ P. Kumar
kumarp@alagappauniversity.ac.in

1 PG & Research Department of Microbiology, Shanmuga Industries Arts & Science College, Tiruvannamalai, Tamil Nadu 606 603, India

2 PG & Research Department of Biotechnology, Mahendra Arts & Science College (Autonomous), Kalippatti, Namakkal, Tamil Nadu 637 501, India

3 Department of Environmental Engineering, Kyungpook National University, 41566 Daegu, Republic of Korea

4 Department of Biomaterials, Saveetha Dental College and Hospital, Saveetha Institute of Medical and Technical Sciences, Chennai 600 077, India

5 Food Chemistry and Molecular Cancer Biology Laboratory, Department of Animal Health and Management, Alagappa University, Karaikudi 630003, Tamil Nadu, India

2021; Suriyakala et al. 2021; Sampath et al. 2021; Heinemann et al. 2021; Swathilakshmi et al. 2022).

Numerous techniques, including hydrothermal, microwave, electrochemical, laser ablation, chemical radiation, ball milling, and green chemistry, have been utilized to create silver nanoparticles (AgNPs) (Aksomaityte et al. 2013; Rabinal et al. 2013; Ellouzi et al. 2021; Ozlem Saygi and Usta 2021). Recently, efforts have been made to design non-toxic and eco-friendly green method for the synthesis of AgNPs. Green chemistry procedures, which are an alternative to chemical and physical processes, have a number of benefits for the synthesis of AgNPs, including reduced time consumption, a slow kinetics ratio, cheap cost, and environmental friendliness. Biological synthesis of AgNPs can be accomplished from plants (Hojjati-Najafabadi et al. 2021) Sengottaiyan et al. 2016; Ameen et al. 2019), bacteria (Ameen et al. 2020), fungi (Popli et al. 2018), actinomycetes (Sowani et al. 2016), cow milk (Lee et al. 2013), panchakavya (Govarthanan et al. 2014), oil cake (Govarthanan et al. 2016a, b), yeast (Korbekandi et al. 2016), and algae (Muthusamy et al. 2017; Gopu et al. 2021). Among these, AgNPs synthesis by marine green seaweeds is more appropriate, since they develop quickly and produce more biomass at a cheaper cost than other organisms. A number of marine seaweeds have been used such as *Gelidium corneum* (Yılmaz Öztürk et al. 2020), *Spyridia filamentosa* (Valarmathi et al. 2020), *Sargassum wightii* (Selvaraj et al. 2020), *Lobophora variegata* (Kitherian et al. 2021), *Ulva armoricana* (Massironi et al. 2019), *Sargassum muticum* (Trivedi et al. 2021), and *Porphyra yezoensis* (Xu et al. 2019) for the reduction of $AgNO_3$ to the synthesis of AgNPs. Seaweeds contain bioactive substances, such as fatty acids, carotenoids, polysaccharides, sterols, and oligopeptides, which have a wide range of biological effects and they perform AgNPs synthesis (Massironi et al. 2019).

In particular, the calcified green seaweed *Halimeda macroloba* genus Halimeda with harder thallus texture due to its high concentration of minerals. Calcium carbonate and bioavailable micronutrients are abundant in Halimeda (Chiarathanakrit et al. 2019). To the best of our knowledge, this is the first report describing the biosynthesis method of AgNPs using green algae, *H. macroloba* extract. The following are the goals of our research: (i) biosynthesis of AgNPs using green seaweed *H. macroloba* extract, (ii) characterization of biosynthesized AgNPs with spectroscopic and electron microscopic methods, (iii) evaluation of in vitro anticancer activity of biosynthesized AgNPs against liver cancer (Huh-7) cells, and (iv) photocatalytic behavior for the degradation of methylene blue (MB) dye was investigated.

Experimental methods and materials

Materials

Silver nitrate ($AgNO_3$) (99.9%), methylene blue (MB), dimethyl thiazolyltetrazolium bromide (MTT), and dimethyl sulfoxide (DMSO) (99.5%) were analytical grades supplied by Himedia Laboratories Pvt. Ltd., (Mumbai, India). All chemicals were used without purification, and deionized water was employed to make solutions. Before being used in research, the glassware was cleaned with deionized water and dried in the hot air oven.

Collection and preparation green seaweed extract

The marine green algae *Halimeda macroloba* was collected from the coastal areas of Tuticorin (Lat. 8.7874°N; Long. 78.1983°E), Tamil Nadu, India. The collected green marine alga was washed with sterile water for four-to-five times to remove epiphytic organisms, necrotic fragments, and other debris. The washed marine alga was shade dried and ground into a fine powder using a domestic grinder. The alga powder (10.0 g) was combined with 100 mL distilled water and heated at 100 °C for 20 min. The algae extract was filtered through Whatman No. 1 filter paper after cooling and stored at 4 °C used for phytochemical analysis and AgNPs' synthesis.

Phytochemical analysis of *H. macroloba*

Phytochemical screening was carried out according to standard procedure described elsewhere (Harborne 1998).

Bioinspired synthesis of AgNPs by *H. macroloba* extract

AgNPs' synthesis was carried out according to Ameen et al. (2019) with slight changes. Briefly, 4 mL of the green algae extract was mixed with 96 mL of 1 mM $AgNO_3$ solution and the resulting greenish mixture was incubated for 24 h at room temperature. The reduction of Ag^+ was seen as a change in color from light green to dark brownish. The pellet was dispersed in double-distilled water and dried in a lyophilizer after centrifugation (Centrifuge, Eppendorf 5810R) at 15,000 rpm for 15 min.

Characterization of AgNPs

The reduction of $AgNO_3$ into AgNPs was investigated using UV–visible spectroscopy (Evolution-201, Thermo, USA). The probable interaction of functional groups

Table 1 Phytochemical screening of *H. macroloba* extract

S. no.	Phytochemicals	Aqueous extract
1.	Alkaloids	–
2.	Phenolic	+ + +
3.	Flavonoids	–
4.	Carbohydrates	+ +
5.	Tannins	+
6.	Saponins	+

+ + + High; + + Medium; + Low; – Absent

involved in the reduction and stability of AgNPs was investigated using Fourier transform infrared (FT-IR; Nicolet iS5, Thermo, USA) spectroscopy. The morphology and size of green-synthesized AgNPs were determined through Transmission electron microscopy (TEM, Tecnai 10, USA) and scanning electron microscope (Jeol JSM 6390 model). In addition, energy-dispersive X-ray (EDX) connected to SEM was used to determine the elemental composition of AgNPs. The size distribution was measured by a laser particle-size analyzer (Nanotrac Wave II, Microtrac Inc, USA). X-ray diffraction (XRD) analysis was performed using a Philips X-pert Pro diffractometer, UK, which was used to study the crystalline state of AgNPs. X-ray photoelectron spectroscopy (XPS, Specs Spectrometer) was used to determine the chemical information on the surface of synthesized AgNPs (Aravinthan et al. 2015).

In vitro cytotoxicity of algae-based AgNPs

MTT (dimethyl thiazolyltetrazolium bromide) assay was used to test the *in-vitro* cytotoxicity of the green algae-based synthesis of AgNPs against breast human hepatoma (Huh-7) cells based on the methodology adopted by Kumar et al. (2014). Briefly, Huh-7 cells (1×10^5 cells/well) were seeded onto the 96-well plates at 37 °C for 24 h. After that, cells were cultured at 37 °C for 24 h with 0–100 g/ml of *H. macroloba* extract and AgNPs. Thereafter, 10 µl of MTT solution (0.5 mg/mL) was added to each well and the incubation period was extended for another 4 h. The formation of purple-colored formazan crystals was slowed by the addition of 100 µl of dimethyl sulfoxide (DMSO) followed by monitoring their absorbance at 590 nm with a microtiter plate reader (Bio-Rad, USA).

Morphological staining

Evaluation of apoptosis by acridine orange and ethidium bromide (AO/EtBr) staining

The morphology and membrane permeability of AgNPs-treated Huh-7 cells were investigated using the AO/EtBr dual staining technique (Puja et al. 2020). Briefly, Huh-7 cells (1×10^5 cells/well) were cultured in 6-well plates and treated for 24 h with AgNPs at a concentration of 90.12 g/

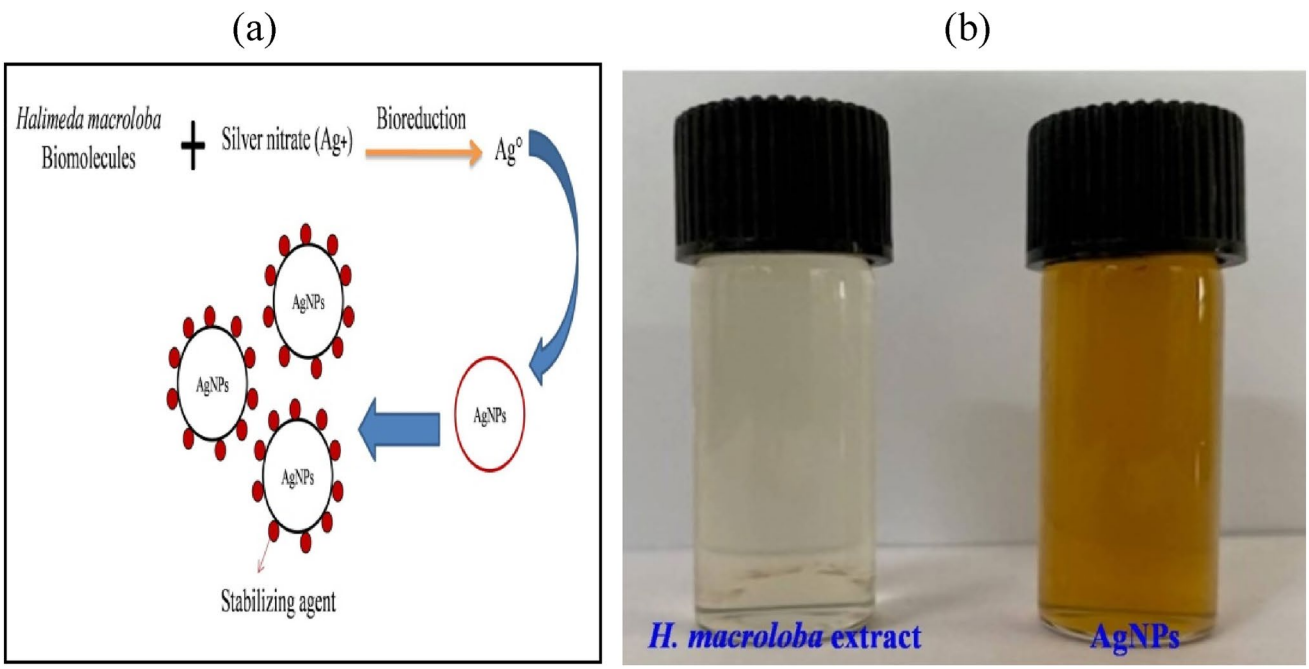

Fig. 1 **a** Bioreduction and stability of AgNPs using *H. macroloba* extract and **b** visual examination of AgNPs formation

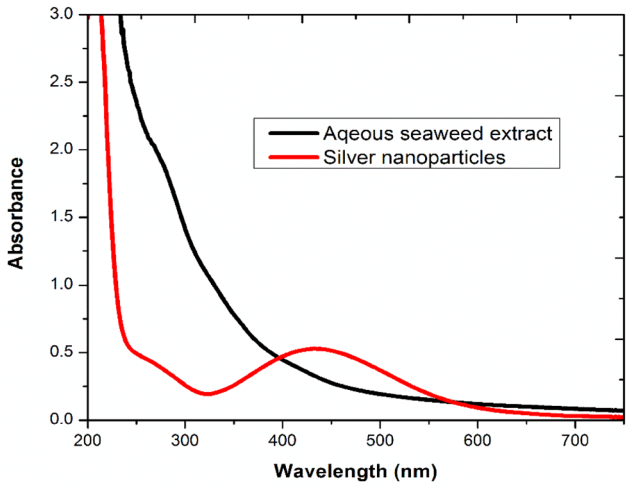

Fig. 2 UV–Vis adsorption spectra of *H. macroloba* extract and AgNPs

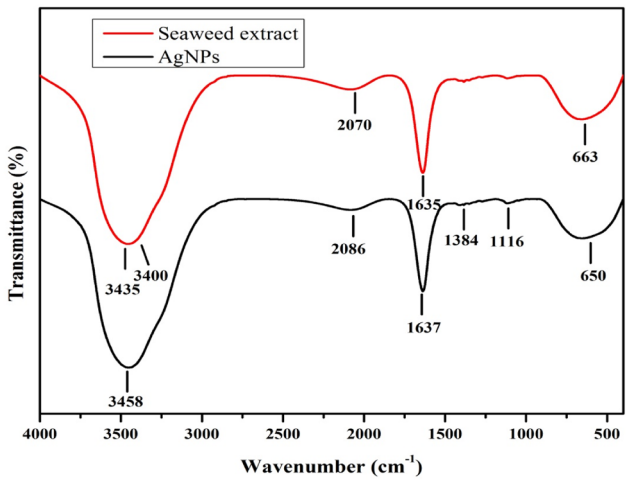

Fig. 3 FT-IR spectrum of *H. macroloba* extract and AgNPs

mL (IC_{50}). The cells were rinsed in phosphate-buffered saline (PBS) and stained with a 2 µL combination of AO/EtBr (100 g/mL) for 5 min after the medium was removed. A fluorescence microscope (Accu-Scope, EX310, USA) was used to examine the cells at a magnification of 20X.

Measurement of intracellular ROS

2′-7′Dichlorofluorescin diacetate (DCFH-DA) staining was used to determine the amount of intracellular ROS activities in Huh-7 cells. Briefly, Huh-7 cells (1×10^5 cells/well) were cultured in 6-well plates and treated for 24 h with AgNPs at a concentration of 90.12 g/mL (IC_{50}). The cells were washed in PBS and stained with 100 µL of DCFH-DA (50 µM) for 15 min under dark. A fluorescence microscope (Accu-Scope, EX310, USA) was used to examine the cells at a magnification of 20X.

Assessment of changes in mitochondrial membrane potential (ΔΨm) (MMP)

Huh-7 cells were cultured and treated for 24 h with AgNPs at a concentration of 90.12 g/ml (IC_{50}). The cells (1×10^5 cells/well) were washed in PBS and stained for 1 h in the dark at 37 °C with rhodamine 123 dye. The mitochondrial membrane potential was examined under a fluorescence microscope (Accu-Scope, EX310, USA).

Photocatalytic degradation of methylene blue (MB) dye

The photocatalytic degradation efficiency of the synthesized AgNPs was assessed by MB with sunlight irradiation (Kayalvizhi et al. 2020). The catalyst AgNPs, weighing about 10 mg, was ultrasonically dispersed in 100 mL of MB for 10 min. The pH and temperature of the dye solution has been observed to be 7.0 and 30 ± 2 °C. The mixed solution was stirred evenly for 30 min in the dark to balance the absorption desorption equilibrium. The solution was sunlight irradiated at given time intervals and extracted in a cuvette to measure the absorption spectrum was estimated using a UV–Vis spectrophotometer (Evolution-201, Thermo, USA). The photocatalytic degradation of MB was monitored at regular intervals of 10 min. The photocatalytic degradation potential of MB was calculated using the following equation:

$$\text{Photodegradation of MB } (\%) = \left(A_0 - A_t/A_t\right) \times 100\%, \quad (1)$$

where A_0 is the adsorption equilibrium concentration of the solution, and A_t is the concentration of solution at time t.

Results and discussion

Phytochemical analysis

A phytochemical screening study was performed to detect the presence of phytomolecules in aqueous leaf extract of *H. macroloba*. Table 1 showed the presence of high phenol, carbohydrates, tannins, and saponins in the aqueous leaf extract of *H. macroloba*. As a result, it is reasonable to assume that phenolic compounds and reducing sugar have a greater capacity to bind Ag^+ ions and may function as a reducing agent, primarily responsible for the bioreduction of Ag^+ to Ag^o and stability of AgNPs (Fig. 1a) (Ramkumar et al. 2017; Arumai Selvan et al. 2018; Govindappa et al. 2021).

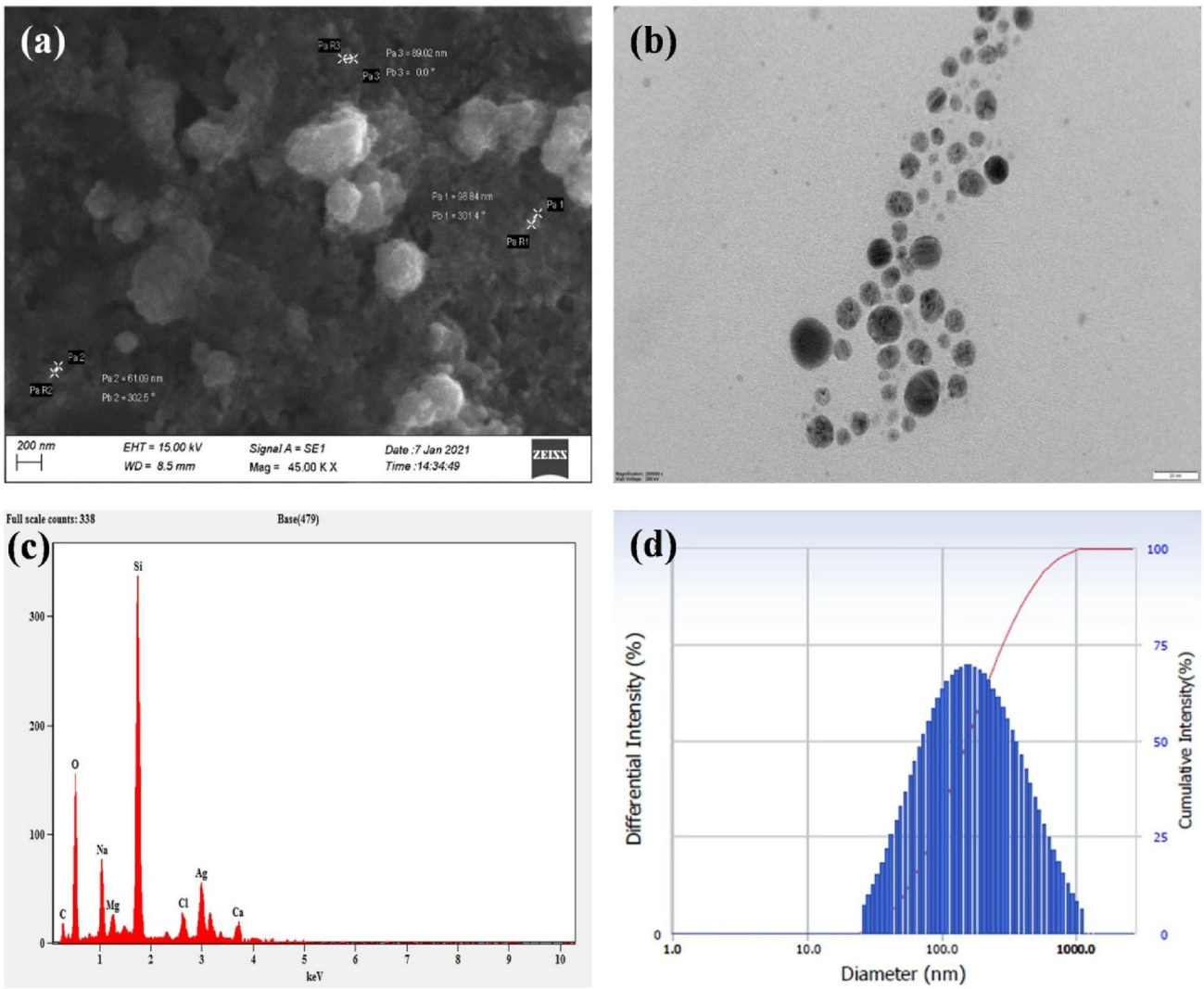

Fig. 4 **a** SEM micrograph, **b** TEM micrograph, **c** EDAX spectrum of Ag, and **d** particle-size histogram of AgNPs

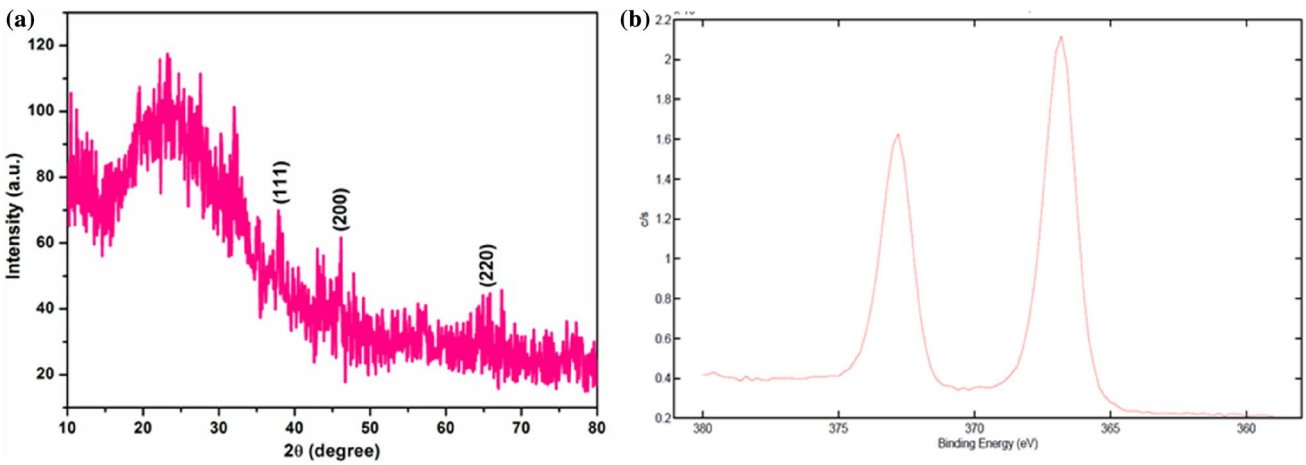

Fig. 5 **a** XRD pattern and **b** XPS spectrum of AgNPs

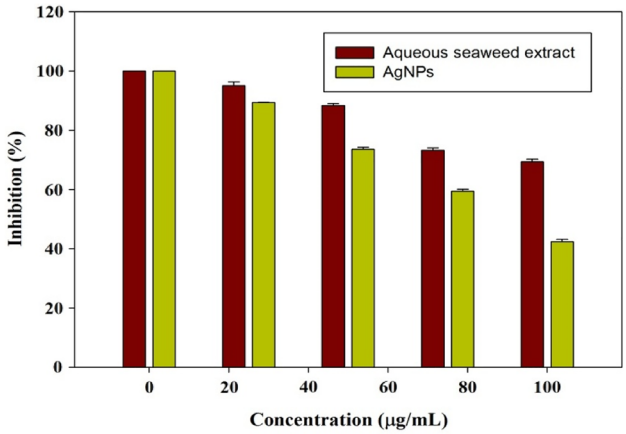

Fig. 6 MTT assay of HUH-7 cells treated with different concentration of synthesized AgNPs

Visual examination of AgNPs

Visual examination of the reaction media revealed the first sign of AgNPs' synthesis. The pale yellow reaction mixture gradually turned dark brown after adding *H. macroloba* extract to $AgNO_3$ solution, indicating the green synthesis of AgNPs (Fig. 1b). The development of a unique dark brown color was caused by the activation of surface plasmon resonance (SPR) in AgNPs (Govarthanan et al. 2014; Mythili et al. 2018; Narayanan et al. 2021). This suggests a high concentration of phenols, carbohydrates, and other phytochemicals that may be involved in the bioreduction of Ag to AgNPs. Several additional reports have verified the same (Gopu et al. 2021; Sampath et al. 2021).

UV–Vis and FT-IR spectral analysis

The green-synthesized AgNPs was confirmed using UV–visible spectroscopy from 200–750 nm. The UV–Vis spectrum of synthesized AgNPs revealed a strong absorbance peak at 420 nm due to the stimulation of SPR (Fig. 2). Several studies have shown that the SPR of AgNPs at 410–440 nm corresponds to spherical shape of AgNPs (Govarthanan et al. 2014; Chinnappan et al. 2018). FT-IR analysis was used to analyze the functional groups contained in *H. macroloba* extract that are responsible for the synthesis of AgNPs. Figure 3 shows that spectrum of *H. macroloba* aqueous extract showed absorbance peaks at 3435 cm^{-1}, 3400 cm^{-1}, 2070 cm^{-1}, 1635 cm^{-1}, and 663 cm^{-1}. The major peaks at 3435 cm^{-1} and 3400 cm^{-1} corresponds to the presence of hydrogen-bonded N–H-stretching vibrations, polyphenolic O–H stretching, respectively (Lakhan et al. 2020; Babu et al. 2020). The strong peak appeared at 1635 cm^{-1} corresponds to the C = C-stretching vibrations of the phenolic group in the extract (Hamedi and Shojaosadati 2019). The spectrum of synthesized AgNPs showed absorbance peaks at 3458 cm^{-1}, 1637 cm^{-1}, 1384 cm^{-1}, 1116 cm^{-1}, and 650 cm^{-1}. The peak appearing at 1637 cm^{-1} corresponds to C = O stretching of carbonyl group that becomes manifest in this range. The shifting and loss of peaks from AgNPs relative to those from *H. macroloba* extract prove the presence of a reaction between the *H. macroloba* and AgNPs (Rajkuberan et al. 2015; Sherin et al. 2020).

SEM, TEM, and PSD characterization

The morphological depiction of synthesized AgNPs was confirmed by SEM micrographs. The SEM micrographs of the AgNPs revealed that they were spherical in form and well dispersed throughout the solution, with aggregation (Fig. 4a). Furthermore, TEM analysis was used to study the surface shape, size, and distribution of the synthesized AgNPs. Figure 4b shows that the green-synthesized AgNPs to be spherical in shape with a size of about 50–100 nm. The biological activity of AgNPs is affected by intrinsic properties, including shape and size. Figure 4c depicts the EDX spectrum at 3 keV, which verified the existence of silver as a significant component element (Lee et al. 2013; Aravinthan et al. 2015; Sengottaiyan et al. 2016; Selvam et al. 2017). Figure 4d shows the particle-size histogram; the average particle size of Ag NPs was determined to be 125.1 nm.

XRD and XPS analysis

X-ray diffraction was used to examine the crystalline structure of the green-synthesized AgNPs (Fig. 5a). The rather wide XRD pattern indicates the synthesized of AgNPs. The XRD patterns of green-synthesized AgNPs show a significant 2 theta peak at 38.53, 44.26, and 67.23 indexed to the plane (111), (200), and (220), respectively. The plane values are consistent with the findings of face-centered cubic structure from JCPDS card number 01–1164. Figure 5b depicts XPS patterns of synthesized AgNPs. The strong binding energy peak of silver was observed at 367.5 eV and 373.8 eV, corresponding to orbital of $3d_{5/2}$ and $3d_{3/2}$, respectively. These peaks shows that Ag (0) is

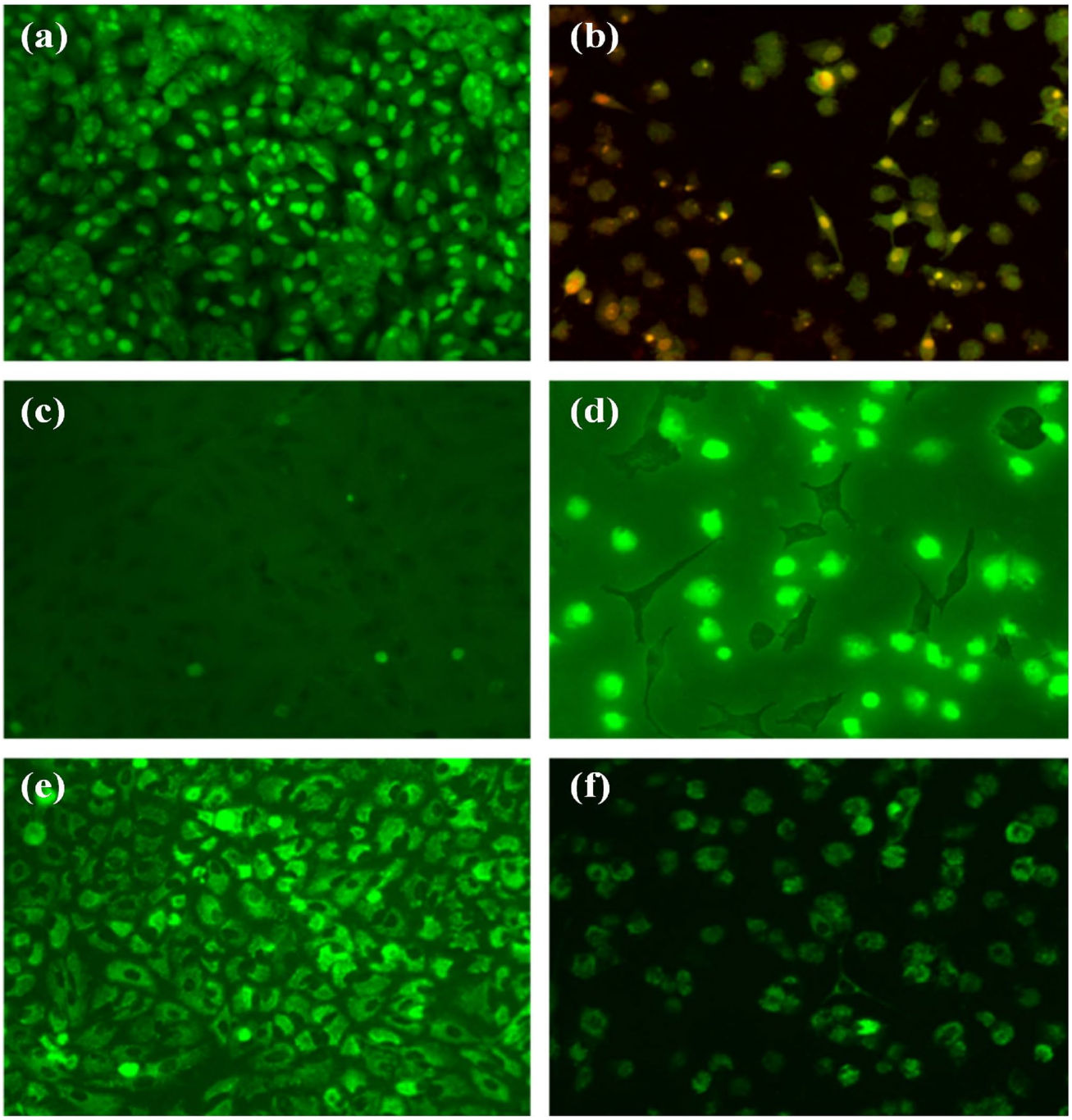

Fig. 7 AO/EtBr stained morphology (**a**) before, (**b**) after AgNPs treated; ROS (**c**) before (**d**) after AgNPs treated; MMP (**e**) before (**f**) after AgNPs treated

the dominant and Ag (I) is completely reduced. The intensity detected in the energy values 367.5 eV and 373.8 eV shows the existence of Ag (0) and Ag (I) (Kumar et al. 2016; Aygün et al. 2020).

In vitro biocompatibility and anticancer activity against Huh-7 cells

The in vitro biocompatibility of green-synthesized AgNPs was checked. The biocompatibility is

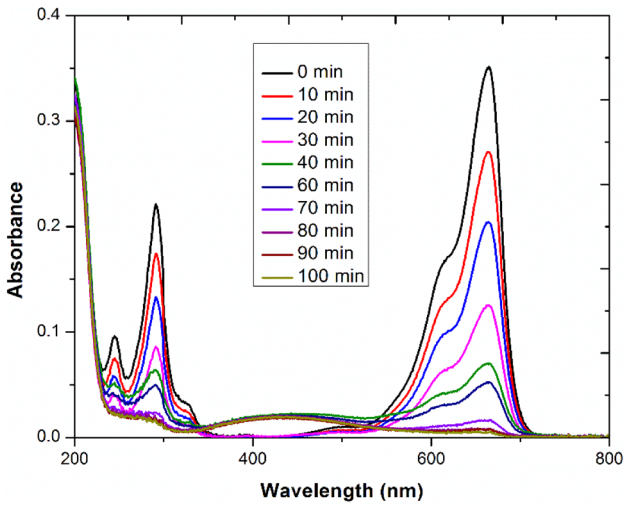

Fig. 8 Photocatalytic degradation of MB

concentration-dependent, with an increase in AgNPs' concentration resulting in a decrease in biocompatibility. Figure 6 shows the effect of green-synthesized AgNPs with different concentrations (0–100 µg/mL) for 24 h onto Huh-7 cells. Cell viability is concentration-dependent, with an increase in AgNPs' concentration resulting in a decrease in cell viability. Biosynthesized AgNPs with an LC_{50} value of 89.5 µg/mL showed significant cytotoxic action. *H. macroloba* aqueous extract alone showed no significant cytotoxic activity against Huh-7 cells. Hence, the AgNPs-treated Huh-7 cells exhibit significant anticancer potential. In a previous work, biosynthesized AgNPs had a dose-dependent anticancer effect on Huh-7 cells (Fageria et al. 2017; Bin-Jumah et al. 2020).

AO/EtBr dual staining methods are commonly used to assess apoptotic changes in cells. Uniform green stained cells signify healthy cells, whereas yellow green granulated granules and orange red cells reflect early and late apoptotic cells, respectively. Figure 7 depicts apoptotic labeling with AO/EtBr which was used to discriminate between living and dead cells. Figure 7a shows the control, the cell nuclei fluoresced consistently green, suggesting that the cells were healthy and the nuclei were intact. Figure 7b shows that the cells treated with AgNPs at IC_{50}, on the other hand, show significant increases in the number of apoptotic cells. The emission of red fluorescence is highly caused by fragmented and condensed DNA within nuclei, implying apoptosis (Puja et al. 2020; Babu et al. 2020; Patel et al. 2021). Figure 7c, d depicts the results of an analysis of the intracellular ROS level in AgNPs-treated cells using the fluorescent dye DCFH-DA. Fluorescence microscopic images revealed increased green fluorescence in cells after treatment with green-synthesized AgNPs. Active mitochondria within cells can be identified with the cationic dye rhodamine 123, which can be easily sequestered by active mitochondria without causing cytotoxicity (Cottet-Rousselle et al. 2011). Figure 7c, d depicts the mitochondrial membrane potential of before and after treated cells with synthesized AgNPs. Treatment with the IC_{50} concentration of synthesized AgNPs resulted in a reduction in ATP generation, indicating the presence of deformed mitochondria (Puja et al. 2020).

Photocatalytic degradation of MB

Figure 8 depicts that the photocatalytic decolorization of MB dye was performed utilizing synthesized AgNPs under direct sunlight irradiation with various incubation times. Under sunlight irradiation, the strength of the absorption peaks progressively declines with increasing duration, with no change in peak location. The highest absorption band of MB in the synthesized AgNPs is around 664 nm (Hamedi and Shojaosadati 2019). This shift in the absorption spectra demonstrates AgNPs' catalytic capability in the degradation of MB to a colorless solution. In less than 100 min, AgNPs degraded MB by about 91.32%. Furthermore, the catalytic capability of produced AgNPs is highly dependent on their size and shape (Ebrahimzadeh et al. 2020; Li et al. 2020; Rajkumar et al. 2021). Comparative data of MB dye degradation by the photocatalyst, AgNPs synthesized using different biological entity including the present work are shown in Table 2. The green-synthesized AgNP is found to be highly efficient photocatalyst in terms of amount of catalyst needed and time taken for degradation of MB dye (Table 2).

Table 2 Comparison of some parameters for degradation of MB using biogenic AgNPs

S. no.	Biological entity	Reaction time (mins)	Degradation efficiency (%)	References
1.	*Chlorella vulgaris*	180	96.51	(Rajkumar et al. 2021)
2.	*Coleus Vettiveroids*	180	70.00	(Ajay et al. 2022)
3.	*Cinnamon bark*	60	97.00	(Aravind et al. 2022)
4.	*Sargassum ilicifolium*	180	100	(Devi et al. 2022)
5.	*Nostoc carneum*	20	92.50	(Borah et al. 2023)
6.	*Halimeda macroloba*	100	91.35	This work

Conclusions

The current work focused on the biogenic, simple, eco-friendly, and cost-effective synthesis of AgNPs utilizing *Halimeda macroloba* aqueous leaf extract. FT-IR spectroscopy indicated the participation of functional groups in the bioreduction of Ag^{+} to Ag^{0}, and UV–Vis spectra show the peak at 430 nm typical of AgNPs. TEM and SEM micrographs confirmed the spherical shape and crystalline nature of the green-synthesized AgNPs. XRD reveals crystalline nature, while the EDX spectrum reveals silver. The green-synthesized AgNPs exhibits higher cytotoxicity activity against Huh-7 cells in a dose-dependent manner. In addition, AgNPs showed apoptosis-associated changes, intracellular ROS changes, and effective mitochondrial membrane potential by AO/EtBr staining, DCFH-DA, rhodamine 123 dye. Furthermore, green AgNPs showed significant catalytic activity in the reduction of MB dye. Overall, green-synthesized AgNPs exhibit a wide spectrum of medicinal and environmental remediation characteristics.

Declarations

Conflict of interest The authors have no relevant financial or non-financial interests to disclose.

References

Ajay S, Panicker JS, Manjumol KA, Parameswaran P (2022) Subramanian, Photocatalytic activity of biogenic silver nanoparticles synthesized using *Coleus Vettiveroids*. Inorg Chem Commun 144:109926

Aksomaityte G, Poliakoff M, Lester E (2013) The production and formulation of silver nanoparticles using continuous hydrothermal synthesis. Chem Eng Sci 85:2–10. https://doi.org/10.1016/j.ces.2012.05.035

Ameen F, Srinivasan P, Selvankumar T et al (2019) Phytosynthesis of silver nanoparticles using *Mangifera indica* flower extract as bioreductant and their broad-spectrum antibacterial activity. Bioorg Chem 88:102970. https://doi.org/10.1016/j.bioorg.2019.102970

Ameen F, AlYahya S, Govarthanan M et al (2020) Soil bacteria Cupriavidus sp. mediates the extracellular synthesis of antibacterial silver nanoparticles. J Mol Struct. https://doi.org/10.1016/j.molstruc.2019.127233

Aravind M, Kumaresubitha T, Ahmed N, Velusamy P (2022) DFT, molecular docking, photocatalytic and antimicrobial activity of coumarin enriched *Cinnamon bark* extract mediated silver nanoparticles. Inorg Chem Commun 146:110176

Aravinthan A, Govarthanan M, Selvam K et al (2015) Sunroot mediated synthesis and characterization of silver nanoparticles and evaluation of its antibacterial and rat splenocyte cytotoxic effects. Int J Nanomedicine 10:1977–1983. https://doi.org/10.2147/IJN.S79106

Arumai Selvan D, Mahendiran D, Senthil Kumar R, Kalilur Rahiman A (2018) Garlic, green tea and turmeric extracts-mediated green synthesis of silver nanoparticles: phytochemical, antioxidant and in vitro cytotoxicity studies. J Photochem Photobiol, B 180:243–252. https://doi.org/10.1016/j.jphotobiol.2018.02.014

Ashraf MA, Peng WX, Fakhri A et al (2019) Manganese disulfide-silicon dioxide nano-material: synthesis, characterization, photocatalytic, antioxidant and antimicrobial studies. J Photochem Photobiol B Biol 198:111579. https://doi.org/10.1016/j.jphotobiol.2019.111579

Aygün A, Gülbağça F, Nas MS et al (2020) Biological synthesis of silver nanoparticles using *Rheum ribes* and evaluation of their anticarcinogenic and antimicrobial potential: a novel approach in phytonanotechnology. J Pharmaceut Biomed Anal 179:113012. https://doi.org/10.1016/j.jpba.2019.113012

Babu B, Palanisamy S, Vinosha M et al (2020) Bioengineered gold nanoparticles from marine seaweed *Acanthophora spicifera* for pharmaceutical uses: antioxidant, antibacterial, and anticancer activities. Bioprocess Biosyst Eng 43:2231–2242. https://doi.org/10.1007/s00449-020-02408-3

Balakrishnan S, Ibrahim KS, Duraisamy S et al (2020) Antiquorum sensing and antibiofilm potential of biosynthesized silver nanoparticles of Myristica fragrans seed extract against MDR *Salmonella enterica serovar Typhi* isolates from asymptomatic typhoid carriers and typhoid patients. Environ Sci Pollut Res 27:2844–2856. https://doi.org/10.1007/s11356-019-07169-5

Behzad F, Naghib SM, Kouhbanani MAJ et al (2021) An overview of the plant-mediated green synthesis of noble metal nanoparticles for antibacterial applications. J Ind Eng Chem 94:92–104. https://doi.org/10.1016/j.jiec.2020.12.005

Bin-Jumah M, AL-Abdan M, Albasher G, Alarifi S (2020) Effects of green silver nanoparticles on apoptosis and oxidative stress in normal and cancerous human hepatic cells in vitro. IJN 15:1537–1548. https://doi.org/10.2147/IJN.S239861

Borah D, Das N, Sarmah P, Ghosh K, Chandel M, Rout J, Pandey P, Ghosh NN, Bhattacharjee CR (2023) A facile green synthesis route to silver nanoparticles using *cyanobacterium Nostoc carneum* and its photocatalytic, antibacterial and anticoagulative activity. Mater Today Commun 34:105110

Chiarathanakrit C, Mayakun J, Prathep A, Kaewtatip K (2019) Comparison of the effects of calcified green macroalga (*Halimeda macroloba Decaisne*) and commercial $CaCO_3$ on the properties of composite starch foam trays. Int J Biol Macromol 121:71–76. https://doi.org/10.1016/j.ijbiomac.2018.09.191

Chinnappan S, Kandasamy S, Arumugam S et al (2018) Biomimetic synthesis of silver nanoparticles using flower extract of *Bauhinia purpurea* and its antibacterial activity against clinical pathogens. Environ Sci Pollut Res 25:963–969. https://doi.org/10.1007/s11356-017-0841-1

Cottet-Rousselle C, Ronot X, Leverve X, Mayol J-F (2011) Cytometric assessment of mitochondria using fluorescent probes. Cytometry A 79A:405–425. https://doi.org/10.1002/cyto.a.21061

Dawood S, Ahmad M, Zafar M et al (2022) Biodiesel synthesis from *Prunus bokhariensis* non-edible seed oil by using green silver oxide nanocatalyst. Chemosphere 291:132780. https://doi.org/10.1016/j.chemosphere.2021.132780

de Jesus RA, de Assis GC, de Oliveira RJ et al (2021) Environmental remediation potentialities of metal and metal oxide nanoparticles: mechanistic biosynthesis, influencing factors, and application standpoint. Environ Technol Innov. https://doi.org/10.1016/j.eti.2021.101851

Devi TA, Sivaraman RM, Thavamani SS, Amaladhas TP, AlSalhi MS, Devanesan S, Kannan MM (2022) Green synthesis of plasmonic nanoparticles using *Sargassum ilicifolium* and application in photocatalytic degradation of cationic dyes. Environ Res 208:112642

Ebrahimzadeh MA, Naghizadeh A, Amiri O et al (2020) Green and facile synthesis of Ag nanoparticles using *Crataegus pentagyna* fruit extract (CP-AgNPs) for organic pollution dyes degradation

and antibacterial application. Bioorg Chem 94:103425. https://doi.org/10.1016/j.bioorg.2019.103425
Ellouzi I, Bouddouch A, Bakiz B et al (2021) Glucose-assisted ball milling preparation of silver-doped biphasic TiO_2 for efficient photodegradation of Rhodamine B: effect of silver-dopant loading. Chem Phys Lett 770:138456. https://doi.org/10.1016/j.cplett.2021.138456
Fageria L, Pareek V, Dilip RV et al (2017) Biosynthesized protein-capped silver nanoparticles induce ROS-dependent proapoptotic signals and prosurvival autophagy in cancer cells. ACS Omega 2:1489–1504. https://doi.org/10.1021/acsomega.7b00045
Gopu M, Kumar P, Selvankumar T et al (2021) Green biomimetic silver nanoparticles utilizing the red algae *Amphiroa rigida* and its potent antibacterial, cytotoxicity and larvicidal efficiency. Bioprocess Biosyst Eng 44:217–223. https://doi.org/10.1007/s00449-020-02426-1
Govarthanan M, Selvankumar T, Manoharan K et al (2014) Biosynthesis and characterization of silver nanoparticles using panchakavya, an Indian traditional farming formulating agent. IJN 9:1593–1599. https://doi.org/10.2147/IJN.S58932
Govarthanan M, Cho M, Park J-H et al (2016a) Cottonseed oilcake extract mediated green synthesis of silver nanoparticles and its antibacterial and cytotoxic activity. J Nanomater. https://doi.org/10.1155/2016/7412431
Govarthanan M, Seo Y-S, Lee K-J et al (2016b) Low-cost and eco-friendly synthesis of silver nanoparticles using coconut (*Cocos nucifera*) oil cake extract and its antibacterial activity. Artif Cells Nanomed Biotechnol 44:1878–1882. https://doi.org/10.3109/21691401.2015.1111230
Govindappa M, Tejashree S, Thanuja V et al (2021) Pomegranate fruit fleshy pericarp mediated silver nanoparticles possessing antimicrobial, antibiofilm formation, antioxidant, biocompatibility and anticancer activity. J Drug Delivery Sci Technol 61:102289. https://doi.org/10.1016/j.jddst.2020.102289
Hamedi S, Shojaosadati SA (2019) Rapid and green synthesis of silver nanoparticles using *Diospyros lotus* extract: evaluation of their biological and catalytic activities. Polyhedron 171:172–180. https://doi.org/10.1016/j.poly.2019.07.010
Harborne AJ (1998) Phytochemical methods a guide to modern techniques of plant analysis, 3rd edn. Springer, Netherlands
Heinemann MG, Rosa CH, Rosa GR, Dias D (2021) Biogenic synthesis of gold and silver nanoparticles used in environmental applications: a review. Trends Environ Anal Chem 30:e00129. https://doi.org/10.1016/j.teac.2021.e00129
Hojjati-Najafabadi A, Salmanpour S, Sen F et al (2022) A tramadol drug electrochemical sensor amplified by biosynthesized Au nanoparticle using *Mentha aquatic* extract and ionic liquid. Top Catal 65:587–594. https://doi.org/10.1007/s11244-021-01498-x
Hojjati-Najafabadi A, Davar F, Enteshari Z, Hosseini-Koupaei M (2021a) Antibacterial and photocatalytic behaviour of green synthesis of Zn0.95Ag0.05O nanoparticles using herbal medicine extract Ceramics International 47: 31617–31624, doi: https://doi.org/10.1016/j.ceramint.2021.08.042
Kayalvizhi S, Sengottaiyan A, Selvankumar T et al (2020) Eco-friendly cost-effective approach for synthesis of copper oxide nanoparticles for enhanced photocatalytic performance. Optik 202:163507. https://doi.org/10.1016/j.ijleo.2019.163507
Kitherian S, Thangapandi V, Jesu Antony MR (2021) Seaweed Lobophora variegata-based silver nanopesticide for environmental friendly management of economically important pest Spodoptera litura. Environ Nanotechnol Monitor Manage 16:100531. https://doi.org/10.1016/j.enmm.2021.100531
Korbekandi H, Mohseni S, Mardani Jouneghani R et al (2016) Biosynthesis of silver nanoparticles using *Saccharomyces cerevisiae*. Artif Cells Nanomed Biotechnol 44:235–239. https://doi.org/10.3109/21691401.2014.937870
Kumar P, Senthamilselvi S, Govindaraju M (2014) Phloroglucinol-encapsulated starch biopolymer: preparation, antioxidant and cytotoxic effects on HepG2 liver cancer cell lines. RSC Adv 4:26787. https://doi.org/10.1039/c4ra02621g
Kumar VA, Uchida T, Mizuki T et al (2016) Synthesis of nanoparticles composed of silver and silver chloride for a plasmonic photocatalyst using an extract from a weed *Solidago altissima* (goldenrod). Adv Nat Sci Nanosci Nanotechnol 7:015002. https://doi.org/10.1088/2043-6262/7/1/015002
Lakhan MN, Chen R, Shar AH et al (2020) Eco-friendly green synthesis of clove buds extract functionalized silver nanoparticles and evaluation of antibacterial and antidiatom activity. J Microbiol Methods 173:105934. https://doi.org/10.1016/j.mimet.2020.105934
Lee K-J, Park S-H, Govarthanan M et al (2013) Synthesis of silver nanoparticles using cow milk and their antifungal activity against phytopathogens. Mater Lett 105:128–131. https://doi.org/10.1016/j.matlet.2013.04.076
Li JF, Liu Y-C, Chokkalingam M et al (2020) Phytosynthesis of silver nanoparticles using rhizome extract of *Alpinia officinarum* and their photocatalytic removal of dye under UV and visible light irradiation. Optik 208:164521. https://doi.org/10.1016/j.ijleo.2020.164521
Massironi A, Morelli A, Grassi L et al (2019) Ulvan as novel reducing and stabilizing agent from renewable algal biomass: application to green synthesis of silver nanoparticles. Carbohyd Polym 203:310–321. https://doi.org/10.1016/j.carbpol.2018.09.066
Muthusamy G, Thangasamy S, Raja M et al (2017) Biosynthesis of silver nanoparticles from Spirulina microalgae and its antibacterial activity. Environ Sci Pollut Res Int 24:19459–19464. https://doi.org/10.1007/s11356-017-9772-0
Mythili R, Selvankumar T, Kamala-Kannan S et al (2018) Utilization of market vegetable waste for silver nanoparticle synthesis and its antibacterial activity. Mater Lett 225:101–104. https://doi.org/10.1016/j.matlet.2018.04.111
Narayanan M, Divya S, Natarajan D et al (2021) Green synthesis of silver nanoparticles from aqueous extract of *Ctenolepis garcini* L. and assess their possible biological applications. Process Biochem 107:91–99. https://doi.org/10.1016/j.procbio.2021.05.008
Ozlem Saygi K, Usta C (2021) Rosa canina waste seed extract-mediated synthesis of silver nanoparticles and the evaluation of its antimutagenic action in Salmonella typhimurium. Mater Chem Phys 266:124537. https://doi.org/10.1016/j.matchemphys.2021.124537
Paiva-Santos AC, Herdade AM, Guerra C et al (2021) Plant-mediated green synthesis of metal-based nanoparticles for dermopharmaceutical and cosmetic applications. Int J Pharm 597:120311. https://doi.org/10.1016/j.ijpharm.2021.120311
Patel P, Nadar VM, Umapathy D et al (2021) Doxorubicin-conjugated platinum theranostic nanoparticles induce apoptosis via inhibition of a cell survival (PI3K/AKT) signaling pathway in human breast cancer cells. ACS Appl Nano Mater 4:198–210. https://doi.org/10.1021/acsanm.0c02521
Popli D, Anil V, Subramanyam AB et al (2018) Endophyte fungi, Cladosporium species-mediated synthesis of silver nanoparticles possessing in vitro antioxidant, anti-diabetic and anti-Alzheimer activity. Artif Cells Nanomed Biotechnol 46:676–683. https://doi.org/10.1080/21691401.2018.1434188
Puja P, Vinita NM, Devan U et al (2020) Fluorescence microscopy-based analysis of apoptosis induced by platinum nanoparticles against breast cancer cells. Appl Organometallic Chem 34:e5740. https://doi.org/10.1002/aoc.5740
Rabinal MK, Kalasad MN, Praveenkumar K et al (2013) Electrochemical synthesis and optical properties of organically capped silver nanoparticles. J Alloy Compd 562:43–47. https://doi.org/10.1016/j.jallcom.2013.01.043

Rajkuberan C, Sudha K, Sathishkumar G, Sivaramakrishnan S (2015) Antibacterial and cytotoxic potential of silver nanoparticles synthesized using latex of *Calotropis gigantea* L. Spectrochim Acta Part A Mol Biomol Spectrosc 136:924–930. https://doi.org/10.1016/j.saa.2014.09.115

Rajkumar R, Ezhumalai G, Gnanadesigan M (2021) A green approach for the synthesis of silver nanoparticles by *Chlorella vulgaris* and its application in photocatalytic dye degradation activity. Environm Technol Innov 21:101282. https://doi.org/10.1016/j.eti.2020.101282

Ramkumar VS, Pugazhendhi A, Gopalakrishnan K et al (2017) Biofabrication and characterization of silver nanoparticles using aqueous extract of seaweed *Enteromorpha compressa* and its biomedical properties. Biotechnol Rep 14:1–7. https://doi.org/10.1016/j.btre.2017.02.001

Sampath G, Govarthanan M, Rameshkumar N et al (2021) Eco-friendly biosynthesis metallic silver nanoparticles using *Aegle marmelos* (Indian bael) and its clinical and environmental applications. Appl Nanosci. https://doi.org/10.1007/s13204-021-01883-8

Sana SS, Li H, Zhang Z et al (2021) Recent advances in essential oils-based metal nanoparticles: a review on recent developments and biopharmaceutical applications. J Mol Liquids 333:115951. https://doi.org/10.1016/j.molliq.2021.115951

Seitkalieva MM, Samoylenko DE, Lotsman KA et al (2021) Metal nanoparticles in ionic liquids: synthesis and catalytic applications. Coord Chem Rev 445:213982. https://doi.org/10.1016/j.ccr.2021.213982

Selvam K, Sudhakar C, Govarthanan M et al (2017) Eco-friendly biosynthesis and characterization of silver nanoparticles using *Tinospora cordifolia* (Thunb.) Miers and evaluate its antibacterial, antioxidant potential. J Rad Res Appl Sci 10:6–12. https://doi.org/10.1016/j.jrras.2016.02.005

Selvaraj P, Neethu E, Rathika P et al (2020) Antibacterial potentials of methanolic extract and silver nanoparticles from marine algae. Biocatal Agric Biotechnol 28:101719. https://doi.org/10.1016/j.bcab.2020.101719

Sengottaiyan A, Mythili R, Selvankumar T et al (2016) Green synthesis of silver nanoparticles using *Solanum indicum* L. and their antibacterial, splenocyte cytotoxic potentials. Res Chem Intermed 42:3095–3103. https://doi.org/10.1007/s11164-015-2199-7

Sherin L, Sohail A, Amjad U-S et al (2020) Facile green synthesis of silver nanoparticles using *Terminalia bellerica* kernel extract for catalytic reduction of anthropogenic water pollutants. Colloid and Interface Sci Commun 37:100276. https://doi.org/10.1016/j.colcom.2020.100276

Sowani H, Mohite P, Munot H et al (2016) Green synthesis of gold and silver nanoparticles by an actinomycete *Gordonia amicalis* HS-11: Mechanistic aspects and biological application. Process Biochem 51:374–383. https://doi.org/10.1016/j.procbio.2015.12.013

Suriyakala G, Sathiyaraj S, Gandhi AD et al (2021) Plumeria pudica Jacq. flower extract - mediated silver nanoparticles: Characterization and evaluation of biomedical applications. Inorg Chem Commun 126:108470. https://doi.org/10.1016/j.inoche.2021.108470

Swathilakshmi AV, Abirami S, Geethamala GV et al (2022) Phytonanofabrication of copper oxide mediated by *Albizia amara* and its photocatalytic efficacy. Mater Lett 314:131911. https://doi.org/10.1016/j.matlet.2022.131911

Trivedi S, Alshehri MA, Aziz AT et al (2021) Insecticidal, antibacterial and dye adsorbent properties of *Sargassum muticum* decorated nano-silver particles. S Afr J Bot 139:432–441. https://doi.org/10.1016/j.sajb.2021.03.002

Valarmathi N, Ameen F, Almansob A et al (2020) Utilization of marine seaweed *Spyridia filamentosa* for silver nanoparticles synthesis and its clinical applications. Mater Lett 263:127244. https://doi.org/10.1016/j.matlet.2019.127244

Wang X, Wang Y, Ying Y (2021) Recent advances in sensing applications of metal nanoparticle/metal–organic framework composites. TrAC Trends Anal Chem. https://doi.org/10.1016/j.trac.2021.116395

Xu Y, Hou Y, Wang Y et al (2019) Sensitive and selective detection of Cu^{2+} ions based on fluorescent Ag nanoparticles synthesized by R-phycoerythrin from marine algae Porphyra yezoensis. Ecotoxicol Environ Saf 168:356–362. https://doi.org/10.1016/j.ecoenv.2018.10.102

Yılmaz Öztürk B, Yenice Gürsu B, Dağ İ (2020) Antibiofilm and antimicrobial activities of green synthesized silver nanoparticles using marine red algae Gelidium corneum. Process Biochem 89:208–219. https://doi.org/10.1016/j.procbio.2019.10.027